Multiple C-Terminal Tails within a Single *E. coli* SSB Homotetramer Coordinate DNA Replication and Repair

Edwin Antony [1,3], Elizabeth Weiland [1], Quan Yuan [2], Carol M. Manhart [2], Binh Nguyen [1], Alexander G. Kozlov [1], Charles S. McHenry [2] and Timothy M. Lohman [1]

*1 - **Department of Biochemistry and Molecular Biophysics,** Washington University School of Medicine, 660 South Euclid Avenue, Box 8231, St. Louis, MO 63110-1093, USA*
*2 - **Department of Chemistry and Biochemistry,** University of Colorado, Campus Box 596, Boulder, CO 80309, USA*

***Correspondence to Timothy M. Lohman:** Fax: +1 314 362 7183. lohman@biochem.wustl.edu*
http://dx.doi.org/10.1016/j.jmb.2013.08.021
Edited by S. Kowalczykowski

Abstract

Escherichia coli single-stranded DNA binding protein (SSB) plays essential roles in DNA replication, recombination and repair. SSB functions as a homotetramer with each subunit possessing a DNA binding domain (OB-fold) and an intrinsically disordered C-terminus, of which the last nine amino acids provide the site for interaction with at least a dozen other proteins that function in DNA metabolism. To examine how many C-termini are needed for SSB function, we engineered covalently linked forms of SSB that possess only one or two C-termini within a four-OB-fold "tetramer". Whereas *E. coli* expressing SSB with only two tails can survive, expression of a single-tailed SSB is dominant lethal. *E. coli* expressing only the two-tailed SSB recovers faster from exposure to DNA damaging agents but accumulates more mutations. A single-tailed SSB shows defects in coupled leading and lagging strand DNA replication and does not support replication restart *in vitro*. These deficiencies *in vitro* provide a plausible explanation for the lethality observed *in vivo*. These results indicate that a single SSB tetramer must interact simultaneously with multiple protein partners during some essential roles in genome maintenance.

Introduction

Single-stranded DNA binding proteins (SSBs) are essential in all kingdoms of life and function in part by binding to the single-stranded DNA (ssDNA) intermediates that form transiently during all aspects of genome maintenance [1,2]. SSB proteins both protect the ssDNA and remove secondary structures, such as hairpins, that can inhibit replication, recombination and repair of DNA. In most bacteria, including *Escherichia coli*, SSB protein functions as a homotetramer with each subunit (177 amino acids in *E. coli*) possessing two domains: a DNA binding domain containing an oligonucleotide/oligosaccharide binding fold (OB-fold) (residues 1–112) and an intrinsically disordered C-terminal tail (65 residues) [3–6]. The last nine amino acids of the C-terminal tail (MDFDDDIPF in *E. coli*) form the site of direct interaction between SSB and more than a dozen other proteins that SSB recruits to their sites of function in DNA replication, repair and recombination [7].

Due in part to its homotetrameric nature, *E. coli* SSB (*Ec*-SSB) can bind to long ssDNA in several DNA binding modes. The dominant binding modes observed *in vitro* are referred to as $(SSB)_{65}$, $(SSB)_{55}$ and $(SSB)_{35}$, where the subscript denotes the average number of nucleotides occluded per SSB tetramer [8–12]. In the $(SSB)_{65}$ mode, favored at high monovalent salt and divalent cation concentrations, ssDNA wraps around all four subunits of the tetramer with a topology resembling the seams of a baseball [5,10]. In contrast, in the $(SSB)_{35}$ binding mode, ssDNA only partially wraps around the tetramer, interacting with an average of only two subunits [8,5,10]. The ssDNA binding properties of these two major binding modes differ significantly. In the $(SSB)_{65}$ mode, an SSB tetramer binds with high affinity, but with little cooperativity [13], yet can undergo random diffusion along ssDNA, a feature

that is important for its ability to transiently destabilize DNA hairpins and facilitate RecA filament formation on natural ssDNA [14,15]. The $(SSB)_{35}$ mode, favored at low salt and high protein-to-DNA ratios, displays extensive positive inter-tetramer cooperativity and thus can form protein clusters or filaments on ssDNA [11,13,16]. In this mode, SSB can undergo a direct or intersegment transfer between ssDNA molecules or distant segments of the same DNA without proceeding through a free protein intermediate [17]. Based on these differences, it has been suggested that the $(SSB)_{35}$ binding mode might function in DNA replication, whereas the $(SSB)_{65}$ binding mode might mediate DNA repair and/or recombination [3,18,19].

DNA replication is a complex process mediated by a replisome containing multiple proteins and enzymes [20], and *Ec*-SSB is a central component of these complexes. The DNA polymerase III holoenzyme (Pol III HE) consists of a DNA Pol III core (α-ε-θ), the multi-subunit DnaX complex clamp loader (τ, γ, δ, δ′, χ and ψ subunits) and the β clamp, a processivity factor. SSB binds to the χψ complex within the clamp loader [21,22] and contributes to processive replication [23,24]. A second interaction of SSB with a Pol III HE site, other than χ, contributes to rapid initiation complex formation in a process where the DnaX complex chaperones Pol III onto β loaded in the same reaction cycle [25]. Recent studies show that leading and lagging strand DNA replication is uncoupled when the SSB–χ interaction is lost [26]. The interaction between SSB and χ is critical as mutations within the protein interaction domain in SSB (e.g., *ssb-113*) are conditionally lethal [27]. Furthermore, strand displacement synthesis catalyzed by the Pol III HE in the absence of helicase is dependent on SSB [28]. SSB directly interacts with primase (DnaG) [29,30] as well as with PriA [22,31]. This latter interaction is critical to the restart of DNA replication at stalled forks and is further enhanced by recruitment of PriB onto DNA [31,32].

Ec-SSB also binds a variety of DNA repair proteins including RecQ (a DNA helicase) [33,34], the RecJ [35] and ExoI nucleases [36]; recombination mediator RecO [37] and DNA Pol IV [38]. Perturbation of the interaction between SSB and these proteins leads to DNA repair defects [39,40]. SSB also interacts with uracil DNA glycosylase [41], a key component of the base excision repair pathway and with repair specific polymerases, DNA Pol II, Pol IV and Pol V, highlighting a role for SSB in translesion DNA synthesis [38,42,43].

Extremophilic bacteria such as *Deinococcus radiodurans* and *Thermus aquaticus* have a dimeric version of SSB [44,45] in which each subunit contains two OB-folds; hence, the DNA binding core still possesses four OB-folds and thus is structurally similar to the homotetrameric SSB. Comparisons of the crystal structures and DNA binding properties of the *Dr*-SSB and *Ec*-SSB suggest that they share similar mechanisms of DNA binding and wrapping [44,46–48]. However, one consequence of the dimeric nature of *Dr*-SSB is that it possesses only two C-terminal tails that can mediate protein–protein interactions.

Whether *E. coli* SSB requires all four C-terminal tails for its functions *in vivo* is not known. To investigate this, we examined the functional consequences of having an SSB with less than four C-terminal tails. We engineered and characterized SSB variants in which either two or all four OB-folds are covalently linked, thus forming a four-OB-fold "tetramer" possessing either only two C-terminal tails [linked SSB dimers (SSB-LD)] or only one C-terminal tail [linked SSB tetramer (SSB-LT)]. We find that a two-tailed SSB "tetramer" (SSB-LD) is functional *in vivo* and is competent for DNA replication *in vitro* but shows defects in DNA repair, and consequently, *E. coli* accumulates significantly more mutations. However, a single-tailed SSB "tetramer" (SSB-LT or SSB-LT-Drl) is unable to complement wild-type (wt) SSB and thus cannot carry out one or more essential functions *in vivo*. This single-tailed SSB also shows defects in coupling leading and lagging strand DNA replication and in replication restart *in vitro*.

Results

Design of covalently linked SSB subunits with two or one C-termini per four OB-folds

wt *Ec*-SSB tetramers contain four OB-folds and four C-termini. To probe the functionality of the four C-terminal tails, we engineered a set of covalently linked SSB proteins that maintain the four OB-folds but possess either only one or two C-termini (Fig. 1a). Our first attempt was to clone two or four *ssb* genes in tandem and remove the appropriate stop codons, generating SSB-linked dimers (SSB-LD) and SSB-linked tetramers (SSB-LT), respectively (Fig. S1). In these constructs, the amino acid linker between two covalently linked OB-folds consisted of the full-length wt C-terminal tail linked directly to the N-terminus of the next OB-fold. We were able to express and purify these recombinant proteins. However, unlike the wt SSB protein that forms a monodisperse homotetramer in solution [3], both the SSB-LD and SSB-LT proteins formed a mixture of oligomeric states (Fig. S2a). Sedimentation velocity analysis of the purified proteins showed multiple broad peaks whose apparent molecular weights corresponded to complexes containing 4 OB-folds, 8 OB-folds, 12 OB-folds and higher (Fig. S2a), suggesting the formation of species in which two or more OB-folds that are covalently linked could be shared to form

higher-order non-covalent complexes. Even though both the SSB-LD and SSB-LT proteins can bind tightly to ssDNA (Fig. S2b), we modified the length and composition of the amino acid linkers between the subunits in an attempt to prevent the formation of these higher-order oligomers.

The SSB protein encoded by *D. radiodurans* (*Dr*) is a homodimer with each subunit containing two OB-folds connected by a 23-amino-acid linker (Fig. 1b) with the sequence QLGTQPELIQ-DAGGGVRMSGAGT [44]. Since this is a naturally occurring linker and because the DNA binding domains of *Ec*-SSB and *Dr*-SSB are structurally similar (Fig. 1b), we used this linker to connect the *Ec*-SSB subunits and generated linked dimer (SSB-LD-Drl) and linked tetramer (SSB-LT-Drl) constructs (Fig. 1a and Fig. S1). Upon expression and purification (Fig. 2a), we found that more than 70–80% of these proteins were single tetramers, and after fractionation over an S200 size-exclusion

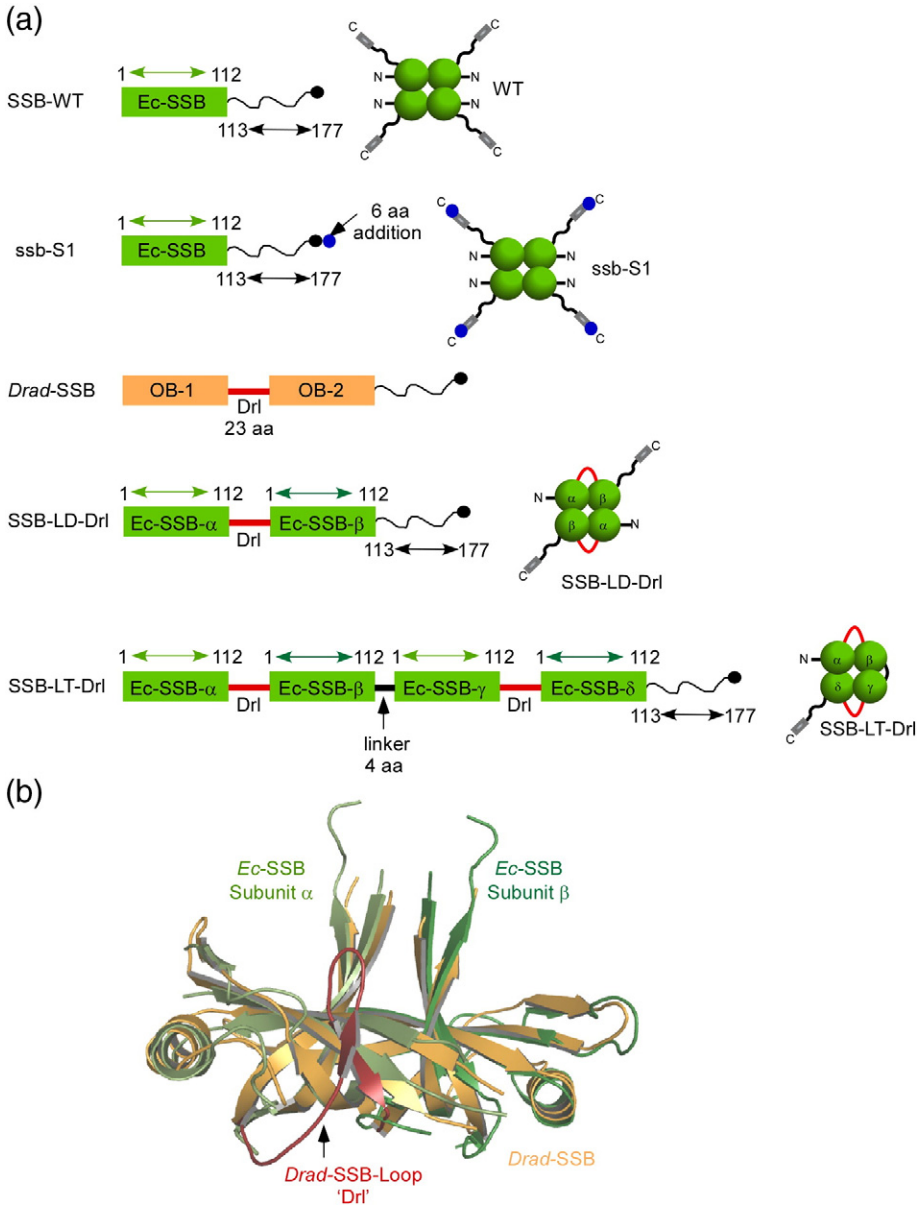

Fig. 1. Design of covalently linked SSB proteins. (a) Schematic of the linker design used to generate the linked SSB dimer (SSB-LD-Drl) and the linked SSB tetramer (SSB-LT-Drl) resulting in two and one C-terminal tail per four OB-folds, respectively. (b) Superimposition of one *Dr*-SSB monomer containing two OB-folds and two *Ec*-SSB subunits containing one OB-fold per subunit. The linker observed between the two OB-folds in the *Dr*-SSB protein is shown in red and is the linker used to design the SSB-LD-Drl and SSB-LT-Drl proteins.

column, we obtained stable versions of both the dimeric SSB-LD-Drl and monomeric SSB-LT-Drl proteins. Sedimentation velocity experiments show that both the dimeric SSB-LD-Drl and monomeric SSB-LT-Drl proteins form single species with apparent molecular weights consistent with the presence of four OB-folds in each construct (Fig. 2b). Further analysis by sedimentation equilibrium revealed a single species for both proteins with average molecular masses of M_r = 65,070 ± 612 Da and M_r = 61,626 ± 112 Da for SSB-LD-Drl and SSB-LT-Drl, respectively (Fig. 2c and d). These values agree with the predicted molecular masses of 67,343 Da for the SSB-LD-Drl (4 OB-folds + 2 C-tails) and 61,266 Da for the SSB-LT-Drl (4 OB-folds + 1 C-tail) based on their amino acid sequences. Once purified, these linked SSB proteins (with either the long or "drl" linker) showed no subunit exchange even after incubation for 3–10 days at room temperature (Fig. S3).

DNA binding properties of covalently linked SSB proteins

We next examined the ssDNA binding properties of the linked SSB proteins. wt SSB binds tightly to ssDNA in a number of distinct DNA binding modes *in vitro*, depending on solution conditions, especially salt concentration and type [3]. On poly(dT), three major ssDNA binding modes are observed at 25 °C, denoted $(SSB)_{35}$, $(SSB)_{55}$ and $(SSB)_{65}$, where the subscript denotes the average number of nucleotides occluded per tetramer [3,8,10]. We therefore measured the average occluded site sizes for the SSB-LD-Drl and SSB-LT-Drl proteins in Buffer T at 25 °C by monitoring the quenching of the intrinsic SSB tryptophan fluorescence upon titrating with poly(dT) at different [NaCl]. Both SSB-LD-Drl and SSB-LT-Drl can form the same three distinct DNA binding modes, $(SSB)_{35}$, $(SSB)_{55}$ and $(SSB)_{65}$, that are observed for wt SSB (Fig. 3a). However, the transitions between the binding modes shift to higher [NaCl] as the number of C-terminal tails decreases from four to two to one. This effect is consistent with previous observations that showed a shift in the $(SSB)_{35}$-to-$(SSB)_{65}$ transition to higher [NaCl] when all four C-terminal tails were truncated by chymotrypsin cleavage [49]. These results indicate that the covalently linked SSB proteins are able to bind and wrap ssDNA to form the same complexes as the wt SSB protein, although the relative stabilities of the different modes are affected.

We also compared the ssDNA binding properties of wt SSB, SSB-LD-Drl and SSB-LT-Drl in the same buffer that we used in the DNA replication assays discussed below [50 mM Hepes, pH 7.5, 100 mM NaCl, 10 mM $Mg(CH_3CO_2)_2$, 100 mM potassium glutamate and 20% (v/v) glycerol] at 25 °C. Under these conditions, we measure similar occluded site sizes of 64 ± 3, 59 ± 4 and 58 ± 3 nt on poly(dT) for the wt SSB, SSB-LD-Drl and SSB-LT-Drl proteins (per four OB-folds), respectively (Fig. 3b). All three proteins also show the same maximum Trp fluorescence quenching. We also examined binding of these proteins to $(dT)_{70}$. wt SSB, SSB-LD-Drl and SSB-LT-Drl all bind tightly to $(dT)_{70}$ with a stoichiometry of one $(dT)_{70}$ molecule per four OB-folds with the same Trp fluorescence quenching consistent with DNA interacting with all four OB-folds with similar wrapping (Fig. 3c). These results indicate that the number of C-terminal tails does not affect the ability of these SSB proteins to form a fully wrapped ssDNA complex. Since SSB binding to $(dT)_{70}$ is stoichiometric under these conditions for all three proteins (i.e., $K_{obs} > 10^9\ M^{-1}$), an accurate estimate of the binding affinities could not be obtained. In order to lower the equilibrium binding constants to the $(dT)_{70}$ substrate to a measureable range, we performed titrations in buffer containing high NaBr concentrations [50] [10 mM Tris–Cl, pH 8.1, 0.1 mM ethylenediaminetetraacetic acid (EDTA) and 1.6 M NaBr] at 25 °C. Under these conditions, the binding affinities of $(dT)_{70}$ for wt SSB, SSB-LD-Drl and SSB-LT-Drl are K_{obs} = $(9 \pm 1.6) \times 10^7\ M^{-1}$, $(9.6 \pm 1.4) \times 10^6\ M^{-1}$ and $(6.6 \pm 0.4) \times 10^6\ M^{-1}$, respectively (Fig. S4). Hence, both linked proteins bind with ~10-fold weaker affinities compared to wt SSB indicating that DNA binding is affected slightly due to the covalent linking of the OB-folds. However, as stated above, under the buffer conditions used to examine DNA replication, all three SSB proteins (wt, LD-Drl and LT-Drl) bind to ssDNA with affinities that are too high to measure and thus ssDNA binding is not compromised.

We also compared the extent to which ssDNA wraps around the four OB-folds in wt SSB, SSB-LD-Drl and SSB-LT-Drl by examining binding to $(dT)_{65}$ labeled with a fluorescence donor (3′-Cy3) and acceptor (5′-Cy5.5) at either end. As shown previously [49,51], when this ssDNA forms a fully wrapped 1:1 molar complex with an SSB tetramer [i.e., in the $(SSB)_{65}$ mode], the two fluorophores are brought into close proximity resulting in a large fluorescence resonance energy transfer (FRET) signal (monitored as a Cy5.5 fluorescence increase). At higher SSB concentrations, two SSB tetramers can bind per DNA, each in the $(SSB)_{35}$ binding mode, resulting in an increase in the distance between the Cy3 and Cy5.5 fluorophores and thus a decrease in FRET signal. Figure 3d shows that we observe the highest FRET signal at a stoichiometry of one $(dT)_{65}$ per "tetramer" (four OB-folds) for all three proteins. At higher SSB concentrations, a second "tetramer" of wt SSB, SSB-LD-Drl and SSB-LT-Drl proteins can bind to the DNA resulting in the expected decrease in FRET.

wt SSB is able to bind two molecules of $(dT)_{35}$ per tetramer, but with negative cooperativity such that the second molecule of $(dT)_{35}$ binds with lower affinity [50,52,53]. Figure 3e compares the binding of $(dT)_{35}$ to wt SSB, SSB-LD-Drl and SSB-LT-Drl proteins in our DNA replication buffer [50 mM Hepes, pH 7.5, 100 mM NaCl, 10 mM $Mg(CH_3CO_2)_2$,

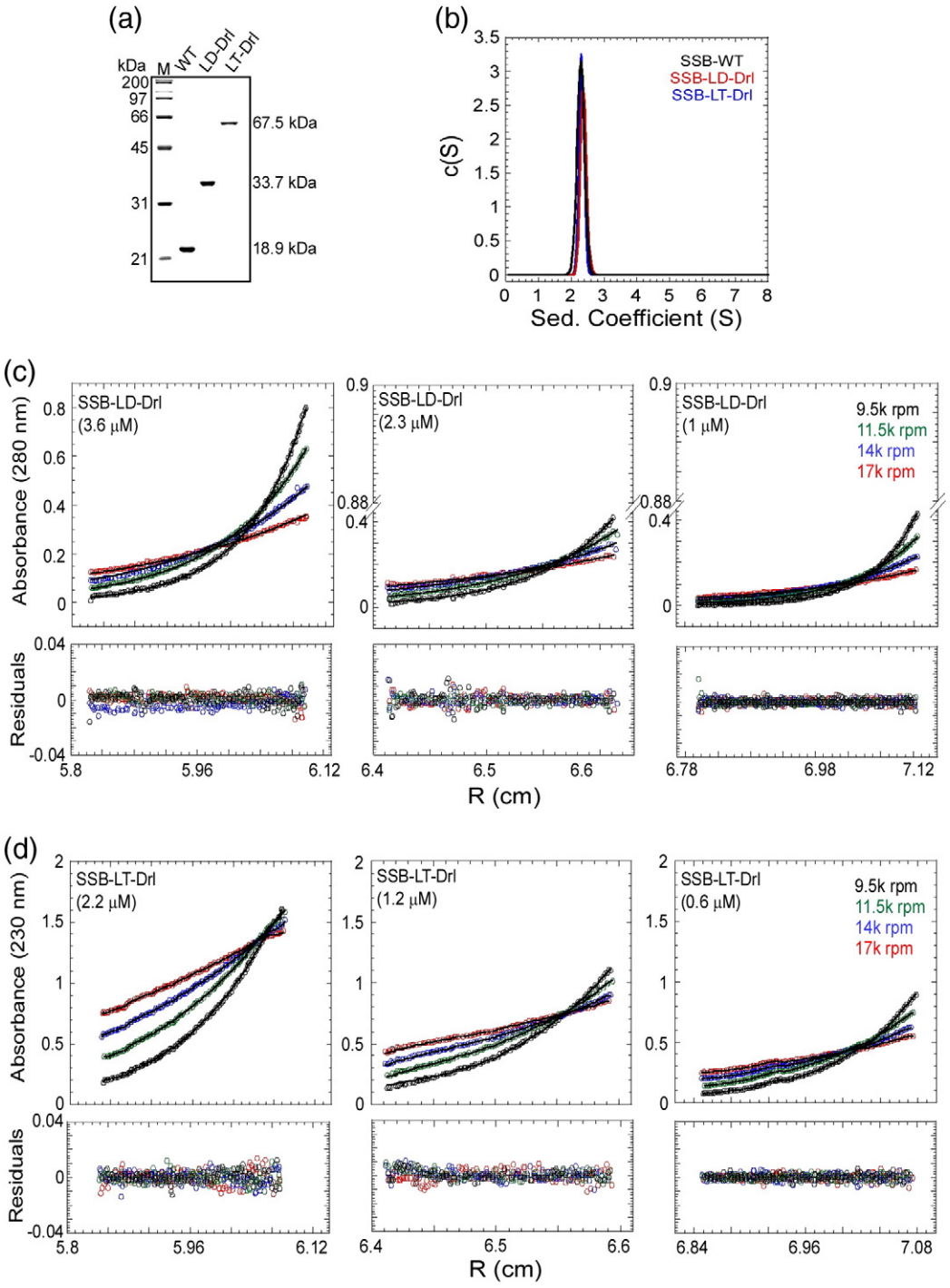

Fig. 2. (a) SDS-PAGE analysis of purified wt SSB, SSB-LD-Drl and SSB-LT-Drl proteins. We analyzed 15 μl of 2 μM protein stocks on a 12% SDS-PAGE gel. (b) Sedimentation velocity analysis of wt SSB, SSB-LD-Drl and SSB-LT-Drl proteins at 42,000 rpm show the presence of a single species in solution for all three proteins. The SSB-LD-Drl (c) and SSB-LT-Drl (d) proteins sediment as tetramers in equilibrium centrifugation experiments with molecular masses corresponding to a single tetramer with four OB-folds (LD-Drl, 65,070 Da; LT-Drl, 61,626 Da). The experiments were performed using three different protein concentrations (as noted) and at four rotor speeds (9500, 11,500, 14,000 and 17,000 rpm). These experiments were performed at 25 °C in buffer containing 30 mM Tris–Cl, pH 8.0, 10% glycerol, 0.2 M NaCl and 1 mM EDTA.

100 mM potassium glutamate and 20% (v/v) glycerol]. Under these conditions, the first $(dT)_{35}$ binds with very high affinity (stoichiometrically), precluding an accurate estimate of the binding constant, whereas the second $(dT)_{35}$ binds with lower binding constants of $(2.34 \pm 0.29) \times 10^5$ M^{-1} and $(1.66 \pm 0.71) \times 10^5$ M^{-1} for SSB-LD-Drl and SSB-LT-Drl proteins, respectively, compared to $(1.60 \pm 0.16) \times 10^7$ M^{-1} for wt SSB (Fig. 3e). The lower affinities of the second $(dT)_{35}$ to the linked proteins are consistent with the observation that the $(SSB)_{35}$ binding mode is favored at higher [NaCl] for these proteins on poly(dT) (Fig. 3a), that is, a

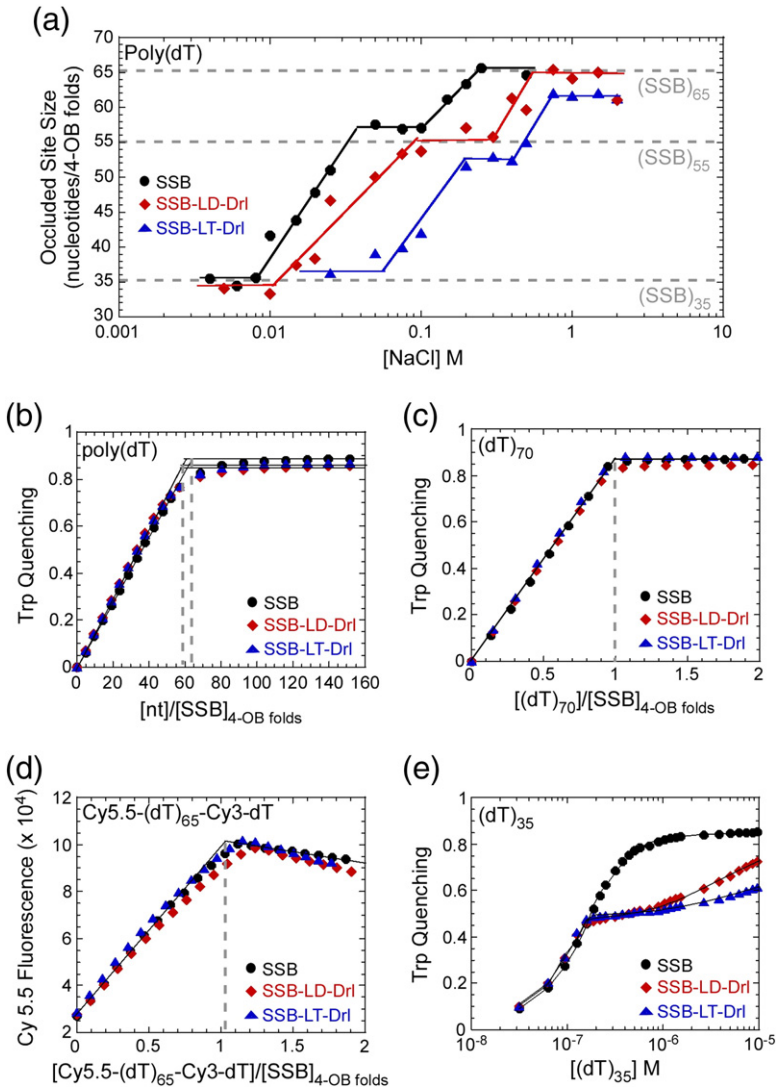

Fig. 3. ssDNA binding properties of linked SSB tetramers. (a) Occluded site size measurements as a function of [NaCl] for the wt SSB and linked SSB proteins on poly(dT) ssDNA show the presence of three distinct DNA binding modes $(SSB)_{35}$, $(SSB)_{55}$ and $(SSB)_{65}$ for all three proteins. (b) Measurement of occluded site size in replication buffer shows that all three proteins bind to ssDNA in the $(SSB)_{65}$ binding mode. (c) Quenching of intrinsic SSB Trp fluorescence upon binding to a $(dT)_{70}$ oligonucleotide shows that all three proteins bind stoichiometrically. (d) Wrapping of ssDNA around wt SSB and linked SSB proteins measured using a oligonucleotide with Cy5.5 and Cy3 fluorophores positioned at the 5′- and 3′-ends, respectively, and monitoring enhancement of Cy5.5 fluorescence at 700 nm by exciting the Cy3 probe at 515 nm. (e) Binding of $(dT)_{35}$ to wt SSB and linked SSB tetramers shows binding of two $(dT)_{35}$ molecules to wt SSB ($K_1 > 10^{15}$ M^{-1} and $K_2 = 1.60 \pm 0.16 \times 10^7$ M^{-1}), both SSB-LD-Drl and SSB-LT-Drl tetramers bind to one $(dT)_{35}$ with high affinity ($K_1 > 10^{15}$ M^{-1} for both SSB-LD-Drl and SSB-LT-Drl) whereas the second $(dT)_{35}$ binding is weaker ($K_2 = 1.66 \pm 0.71 \times 10^5$ M^{-1} and $2.34 \pm 0.29 \times 10^5$ M^{-1} for SSB-LD-Drl and SSB-LT-Drl, respectively). The experiments in panels b, c, d, and e were performed at 25 °C in buffer containing 50 mM Hepes (pH 7.5), 10 mM $Mg(OAc)_2$, 100 mM NaCl, 100 mM $KC_5H_8NO_4$ and 20% glycerol.

higher [NaCl] is required for these proteins to shift from the lower site size binding mode to the higher site size binding mode.

Recent single molecule fluorescence studies have shown that an *Ec*-SSB tetramer is able to diffuse along ssDNA [49] and that it uses this property to transiently melt a double-stranded DNA hairpin and that this activity of SSB can facilitate formation of a RecA filament on natural ssDNA [15]. Using these same single molecule approaches, we show (Fig. S5) that the covalently linked SSB proteins are also able to diffuse along ssDNA and transiently melt a DNA hairpin.

An SSB with at least two C-terminal tails is required for *E. coli* survival

We next examined the ability of the covalently linked SSB proteins, SSB-LD-Drl and SSB-LT-Drl, to function in *E. coli* by testing their ability to complement the loss of wt SSB protein *in vivo* using a "bumping" assay developed by Porter [54]. *E. coli* strain RDP317 lacks a chromosomal copy of the wt *ssb* gene and thus can survive only if it also carries a plasmid expressing a version of an *ssb* gene that can functionally complement the *wt ssb* gene. We first grew RDP317 cells containing a plasmid expressing the *wt ssb* gene (pRPZ150; reclassified in Table S1 as pEW-WT-*t*) that also contains a tetracycline resistance cassette (tet^R). The *ssb* mutant gene to be tested for complementation was then cloned into a second compatible plasmid containing ampicillin resistance (amp^R) (pEW-X-*a*; where "X" denotes the SSB variant to be tested and "*a*" denotes the resistance to ampicillin; Table S1). We cloned each *ssb* gene under control of the natural *ssb* promoter to regulate expression levels of all SSB constructs [55,56]. RDP317 cells containing the pEW-WT-*t* (ssb^+, tet^+) were then transformed with the test plasmid (pEW-X-*a*). The transformed cells were then passaged (sub-cultured successively) five to six times, selecting for cells possessing ampicillin resistance (100 μg/ml ampicillin). If the test *ssb-x* gene is able to complement wt *ssb*, the plasmid containing the wt *ssb* gene along with its tet^R cassette can be lost (bumped) from RDP317. However, if the test gene is unable to complement wt *ssb*, then the original (ssb^+, tet^+) plasmid will be retained in RDP317. Consequently, if a test *ssb-x* gene complements the wt *ssb* gene, then cells containing the test *ssb-x* gene will possess only ampicillin resistance, whereas if the test *ssb-x* gene does not complement the wt *ssb* gene, then cells containing the test *ssb-x* gene will be resistant to both ampicillin and tetracycline. Our results indicate that the *ssb-LD-Drl* gene expressing SSB with only two C-tails is able to functionally complement the loss of wt *ssb* gene *in vivo*; however, the *ssb-LT-Drl* shows a dominant lethal phenotype (Table 1; discussed below).

The last nine amino acids of the SSB C-tail provides the site of interaction of SSB with more than one dozen SSB interacting proteins (SIPs), and this site is critical for SSB function as *ssb* genes with deletions of the last eight amino acids (*ssb-ΔC8*) [57] or that contain an additional six-amino-acid extension (*ssb-S1*) do not complement loss of the wt *ssb* gene (Table 1). The genes encoding for covalently linked SSB proteins possessing only two C-tails (*ssb-LD* and *ssb-LD-Drl*) complement the wt *ssb* gene (Table 1). To check the integrity of the genes encoding the linked SSB proteins, we isolated plasmid DNA after the final passage. Sequencing of the *ssb-LD-Drl* gene showed the expected sequence with no evidence of mutations or recombination events. Occasionally, we observed recombination events within the *ssb-LD* gene that uses the wt SSB C-terminus to link the two subunits. However, all complementation results that we report here for *E. coli* containing the *ssb-LD* or *ssb-LD-Drl* genes are for genes whose sequence was verified. The absence of the wt SSB protein in these cells after bumping was also confirmed by Western blot analysis (Fig. S6). Hence, two functional C-terminal tails within an SSB construct containing four OB-folds are sufficient to support *E. coli* growth. However, neither of the genes encoding *ssb-LT* or *ssb-LT-Drl*, expressing SSB with only one C-tail, were able to complement and in fact were toxic indicating a dominant lethal phenotype (Table 1). We were able to successfully clone these constructs into plasmids under control of a T7 promoter, but multiple attempts to clone them under control of the native SOS promoter were unsuccessful. For both the *ssb-LT* and *ssb-LT-Drl* constructs, only a few colonies appeared after transformation, but in every case (total of 9 colonies from 8 attempts), the genes contained mutations that introduced premature stop codons within the open reading frame. These results suggest that an SSB tetramer with one free tail is toxic to *E. coli* when under the control of the SOS promoter.

Since the *ssb-LD-Drl* gene was able to support cell growth, we also tested whether the *Dr-ssb* gene (which encodes a naturally occurring two C-tail protein in *D. radiodurans*) can functionally complement *wt*

Table 1. Results of *ssb* Complementation (Bumping) Assay

Construct	Phenotype
Unlinked monomers	
wt	Complements
SSB-S1	No complementation
Linked dimer	
SSB-LD	Complements
SSB-LD-Drl	Complements
Linked tetramers	
SSB-LT	Dominant lethal
SSB-LT-Drl	Dominant lethal

ssb. The nine C-terminal amino acids of the *Dr*-SSB protein are PPEEDDLPF, which is similar to the MDFDDDIPF sequence found in the *Ec*-SSB protein. In fact, *Dr*-SSB is able to complement wt SSB protein *in vivo* (Table S1) and as shown previously [47], providing additional evidence that an SSB with only two C-terminal tails is sufficient to allow *E. coli* survival and growth.

SSB with fewer than four C-terminal tails exhibits decreased stimulation of the DNA polymerase III holoenzyme on single-stranded templates

We next examined whether the linked SSB constructs could function in *E. coli* DNA replication. We first examined the simple conversion of primed ssDNA to a duplex (Fig. 4a). This reaction requires the ability of the Pol III HE to form an ATP-dependent initiation complex on a primer and to processively elongate it approximately 8000 nt. The reaction is independent of SSB under low salt conditions but becomes partially (~3- to 4-fold) dependent upon SSB at elevated salt concentrations (200 mM NaCl). We observe full stimulation of the reaction by wt SSB and incrementally less stimulation by SSB-LD-Drl and SSB-LT-Drl, respectively (Fig. 4a). The level of DNA synthesis observed in reactions containing one-tailed SSB-LT-Drl is only slightly above that observed in the absence of SSB.

As expected, SSB-S1, an SSB homotetramer that possesses four C-terminal tails but with a six-amino-acid extension after the nine-amino-acid SIP interaction sequence severely inhibits the reaction (Fig. 4a). Extensions of the amino acid sequence beyond the normal C-terminal phenylalanine have been shown to block SIP interactions [22,30], and we have shown that the SSB-S1 protein does not interact with χ (Fig. S7). We have previously observed inhibition by other SSB derivatives that lack portions of the C-terminal tail [28].

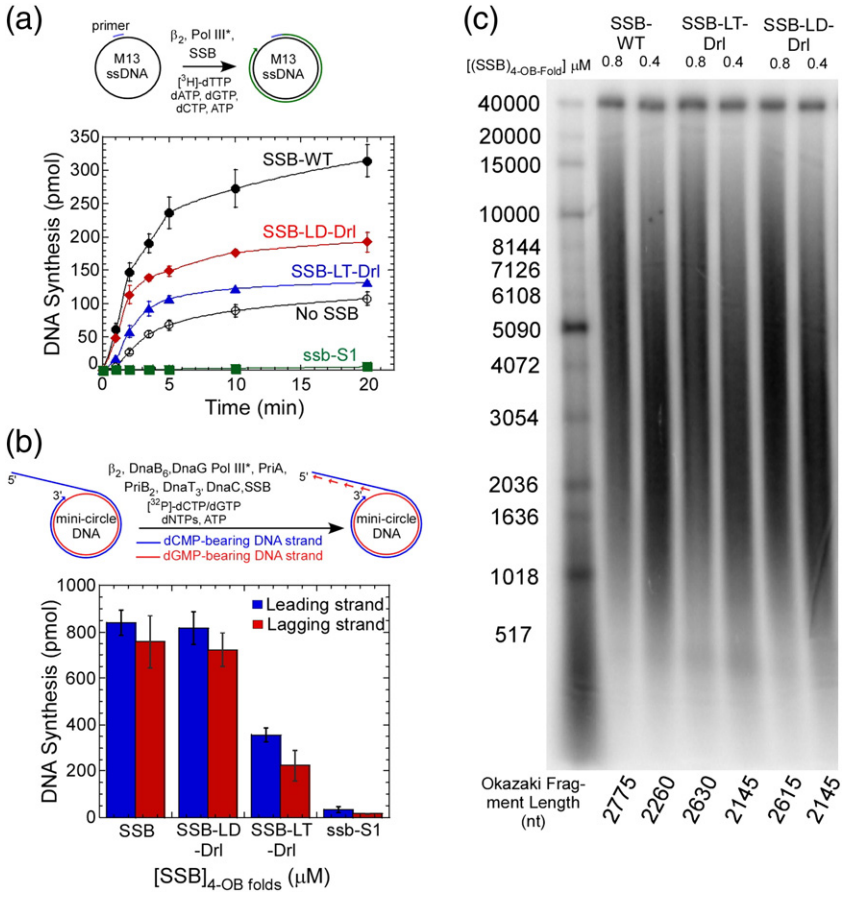

Fig. 4. Linked SSB tetramers with only one C-terminal tail show decreased stimulation of DNA replication. (a) *In vitro* ssDNA replication assays were carried out in the presence of the indicated SSB derivative. (b) *In vitro* rolling circle DNA replication assays were carried out in the presence of the indicated SSB derivative. (c) The products from the rolling circle replication reactions were fractionated on an alkaline agarose gel, and the length of Okazaki fragments was determined. (From left to right: 2775, 2260, 2630, 2145, 2615 and 2145 nt.)

SSB containing only one C-terminal tail is defective in rolling circle replication reactions that mimic chromosomal replication forks

Duplex circles containing a 5′-flap on one strand provide a substrate for reconstitution of replication forks that exhibit the same characteristics of replication forks *in vivo* [58]. In this case, replication is dependent upon restart primosomal proteins (PriA, PriB, DnaT) that direct the assembly of the DnaB helicase in the presence of the DnaC helicase loader and SSB. Once the helicase is loaded on the lagging strand template, it uses its ATP-dependent DNA helicase activity to unwind the duplex DNA at the replication fork, permitting the dimeric Pol III HE (associated with DnaB through an interaction with the τ subunit of Pol III HE [59,60]) to follow. Primers are provided on the lagging strand by a reversible interaction between the DnaG primase and DnaB [61,62]. The lagging strand primers are extended by the lagging strand half of the dimeric Pol III HE in a coupled reaction [60].

We find that SSB-LD-Drl functions equivalently to wt SSB in this system. However, SSB-LT-Drl, containing only one C-tail, exhibits a 2-fold decrease in the level of leading strand synthesis (Fig. 4b). The levels of lagging strand synthesis are decreased even further, suggesting that leading and lagging strand DNA replication reactions become uncoupled.

To determine whether the decrease in lagging strand synthesis relative to leading strand is due to a defect in primer formation, we examined Okazaki fragment length by electrophoresis of labeled lagging strand products in alkaline agarose gels (Fig. 4c). We observe similar product lengths with all three proteins (wt SSB, SSB-LD-Drl and SSB-LT-Drl) suggesting that the replication defect is not associated with formation of primers. Uniform Okazaki fragment length is an indication that primers are synthesized with the same frequency and spacing in the presence of all three SSB proteins [63].

A one-tailed SSB tetramer does not support replication restart

In the rolling circle replication reactions described above, the initial PriA-dependent helicase assembly occurred during a 5-min pre-incubation of components in the presence of ATPγS. This precluded use of the rolling circle reactions to examine the effect of the SSB variants on the kinetics of the replication restart reaction. We therefore used a recently developed FRET assay that monitors PriA- and SSB-dependent helicase assembly on model forks [64]. Unwinding activity in this experiment is a direct measure of DnaC's helicase loading onto the leading strand. The presence of the streptavidin-biotin complex on the 5′-end of the lagging strand prevents helicase loading at that site. SSB is required for the loading of the DnaB helicase onto the leading strand primer-template. Using this assay under conditions where DNA unwinding is proportional to the time of the reaction, we observe a modest decrease in DNA unwinding when SSB-LD-Drl is substituted for SSB. However, substitution with the one-tailed SSB-LT-Drl results in a severe inhibition of the unwinding reaction indicating an inability of the single-tailed SSB to load the DnaB helicase. The level of inhibition is nearly equivalent to that observed with the SSB-S1 derivative (Fig. 5).

E. coli cells expressing two-tailed SSB tetramers are more resistant to DNA damage but accumulate more mutations

Since *Ec*-SSB interacts with several proteins involved in DNA repair [7,33,65], we tested whether the number of C-tails associated with a single SSB tetramer affects the ability of cells to recover from DNA damage. *E. coli* cells expressing either wt SSB or SSB-LD-Drl were grown in the presence of the DNA damaging agents hydroxyurea (HU) and nitrogen mustard [$N(CH_2CH_2Cl)_3$ or HN2] or exposed to UV irradiation. HU is an inhibitor of ribonucleotide reductase, and treatment of *E. coli* results in depletion of dNTP pools leading to DNA double-strand breaks near replication forks [66,67], whereas HN2 inhibits DNA replication by covalently cross-linking the two DNA strands [68]. Exposure of cells to UV irradiation leads to formation of DNA breaks, base damage and UV sensitivity [69]. To assess the ability of a four-tailed *versus* two-tailed SSB to respond to DNA damage, we grew cells carrying these genes in the presence of either HU (100 mM) or HN2 (2 mM). We then compared the relative abilities of the cells to grow after exposure to these DNA damaging agents. Surprisingly, cells expressing the two-tailed SSB-LD-Drl recover faster from exposure to both DNA damaging agents as indicated by faster cell growth observed across the serial dilutions (Fig. 6a and b).

To test the ability of the RDP317 cells carrying either the *wt ssb* or the *ssb-LD-Drl* genes to recover from UV-induced damage, we grew overnight cultures, plated serial dilutions of these cells and exposed them to varying levels of UV irradiation. *E. coli* cells expressing either wt SSB or SSB-LD-Drl display comparable sensitivities to low levels of UV irradiation (0–25 J/m^2) as indicated by the growth of the colonies across the serial dilutions (Fig. 6c). However, after exposure to higher UV levels (150 J/m^2), the cells expressing SSB-LD-Drl show a slight recovery, compared to the failure of cells expressing wt SSB to recover from these high UV doses (Fig. 6d).

Since one of the major proteins expressed in response to DNA damage is RecA, we hypothesized that the ability of the cells expressing SSB-LD-Drl to better recover from the effects of DNA damage might be due to expression of higher

levels of RecA. To test this, we treated cells with nalidixic acid (a DNA damaging agent) and quantified the expression levels of RecA using an anti-RecA antibody. However, Western blots (Fig. 6e) show a similar level of induction of RecA protein in the presence of nalidixic acid for cells expressing either wt SSB or SSB-LD-DrI.

Another possible explanation for the faster recovery of the SSB-LD-DrI cells after DNA damage is that the DNA lesions are not repaired, but bypassed. If this were the case, then an elevated rate of mutagenesis should occur in these cells. We thus compared the rate of mutagenesis in these cells using the rifampicin resistance assay [70]. *E. coli* grown in the presence of rifampicin can survive through spontaneous mutations in the rifampicin binding site on the β subunit of RNA polymerase. We observe a 30-fold increase in the number of *Rif*^{r} colonies in the SSB-LD-DrI cells compared to the wt SSB cells (Fig. 7a). These results suggest that the better recovery from the effects of the DNA damaging agents are due to a lower level of repair of DNA in cells expressing SSB-LD-DrI. Repair of mutations after DNA damage results in slower cell growth [71]. Since cells expressing SSB-LD-DrI are deficient in repairing mutations, we would expect these cells to display faster growth kinetics. The data in Fig. 7 (b and c) show this to be the case as cells expressing SSB-LD-DrI enter exponential growth phase significantly faster than cells expressing wt SSB. When cell growth is initiated from overnight cultures, cells expressing SSB-LD-DrI reach the mid-log phase about 70 min faster than cells expressing wt SSB (Fig. 7b). When cell growth is initiated from cells in log phase, the SSB-LD-DrI cells reach mid-log about 120 min faster than the wt SSB cells (Fig. 7c). These results support the conclusion that the SSB-LD-DrI protein with two C-tails per tetramer promotes defects in DNA repair but is able to support DNA replication.

Discussion

In addition to its role in binding ssDNA, *E. coli* SSB protein serves as an important recruitment platform during DNA replication, repair and recombination in that it binds more than a dozen proteins (SIPs) via its unstructured C-terminal tails. Each SSB homotetramer has four potential SIP binding sites, and we show here that a reduction in the number of C-terminal tails associated with each tetramer has deleterious effects on many of its biological functions. We find that *E. coli* cells are unable to survive when expressing an SSB construct that contains four OB-folds ("tetramer") but only one C-terminal tail (SSB-LT-DrI), whereas *E. coli* expressing an SSB "tetramer" with only two tails (SSB-LD-DrI or *Drad* SSB) is able to survive. Furthermore, whereas a two-tailed SSB "tetramer" is able to coordinate leading and lagging strand DNA replication *in vitro*, a single-tailed "tetramer" is deficient *in vitro*. In addition, the single-tailed SSB does not support the loading of the DnaB helicase in a model replication restart assay, whereas a two-tailed SSB can function in this capacity. However, even though the two-tailed SSB "tetramer" can support cell growth, this variant shows defects in DNA repair, and as a consequence, mutations accumulate at a high frequency. These results indicate that more than one tail is needed within a single SSB tetramer for it to properly function in at least one essential process *in vivo*. Therefore, either a single SSB tetramer is required to bind to at least two SIP proteins simultaneously or one essential SIP interacts simultaneously with two C-terminal tails on a single SSB tetramer.

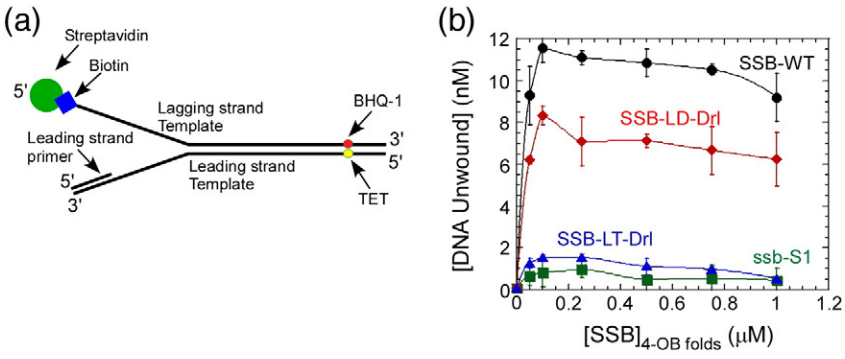

Fig. 5. SSB-LT-DrI does not support PriA-dependent replication restart pathway. (a) DNA substrate used in unwinding reactions. The fluorescence of TET on the 5′-terminus increases when separated by helicase action from a quencher (BHQ-1) on the lagging strand template. Streptavidin binding to biotinylated thymidine on the 5′-end of the lagging strand template blocks DnaB helicase self-loading by threading over a free 5′-end. There is a 10-nt gap between the 3′-OH of the leading strand primer and the duplex region of the fork. (b) SSB variants titrated individually in triplicate in the presence of 150 nM PriA, 50 nM $PriB_2$, 50 nM $DnaT_3$, 12 nM $DnaB_6$ and 50 nM DnaC.

In an attempt to reconcile the dominant lethal phenotype of *ssb-LT-Drl* with *in vitro* biochemical observations, we examined the consequence of substituting wt SSB with the SSB-LD-Drl and SSB-LT-Drl derivatives in DNA replication assays. In an assay where the processive activity of Pol III HE is required for efficient conversion of an 8000-nt single-stranded circle to a duplex, we observed a decrease in the ability of the SSB derivatives with one or two tails to stimulate this reaction. The reduced velocities can be explained by fewer DNA molecules participating in the reaction. Thus, at least part of the defect appears to be in the initiation phase of the reaction. The χ subunit of the Pol III HE interacts with the C-terminal tail of SSB and facilitates binding to and elongating templates that are coated with SSB [21–24]. We have observed that an interaction between a Pol III HE component other than χ and the C-terminal tail of SSB is required for the optimal efficiency of initiation complex formation under conditions where Pol III associated with τ-containing DnaX complexes is chaperoned onto newly assembled β [25]. During initiation complex formation in the presence of single-tailed SSB-LT-Drl, it is possible that a portion of the Pol III HE interacts through χ precluding stimulation by the second interaction site or even trapping the enzyme in a non-productive complex.

In a more complex rolling circle replication reaction, we observe no difference upon substituting the two-tailed SSB (SSB-LD-Drl) for wt SSB; however, a 2-fold decrease in leading strand synthesis and a further decrease in lagging strand synthesis is observed upon substituting the one-tailed SSB, SSB-LT-Drl. In this assay, a dimeric Pol III HE simultaneously replicates the leading and lagging strand in a reaction that is coupled, in part, through an interaction with the DnaB helicase [59,60]. The decrease in leading strand synthesis could be explained by a defect in interaction of the Pol III HE through χ to SSB coating the lagging strand. This interaction has been shown to be important for stabilizing leading strand replication during the

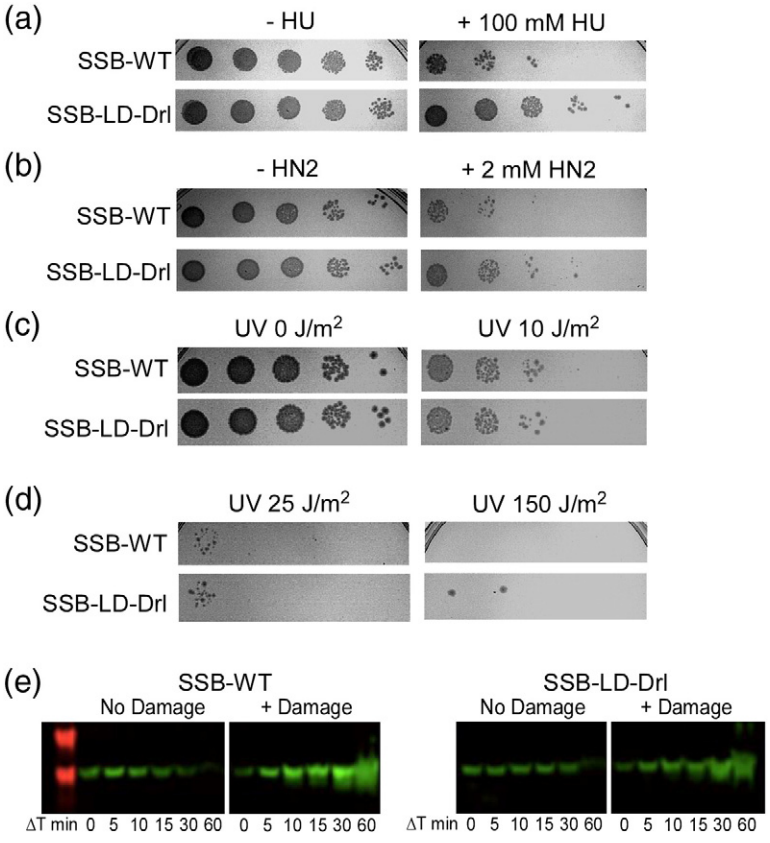

Fig. 6. *In vivo* repair capabilities of *E. coli* strains carrying *wt SSB* or *ssb-LD-Drl* genes. Serial dilutions of cells in the absence or presence of 100 mM HU (a) or 2 mM nitrogen mustard (b). Cells harboring the *ssb-LD-Drl* gene recover better compared to the wt cells in the presence of either DNA damaging agent. Both strains tolerate lower levels of UV to similar extents (c). However, at a higher dose of UV (d), only the cells carrying the *ssb-LD-Drl* gene able to grow. (e) Western blot detection of RecA levels in the absence or presence of 100 mM nalidixic acid. Both strains are capable of inducing RecA expression in the presence of DNA damage.

extensive elongation that takes place on rolling circle templates [26] and in stabilizing leading strand Pol III HE in strand displacement reactions [28].

The additional lagging strand defect was not due to slower, lagging-strand-specific elongation or a defect in priming, as the lengths of the Okazaki fragments produced, which is sensitive to Pol III HE elongation rates and the frequency of primer synthesis and utilization [72], were the same in all cases. The additional decrease in lagging strand synthesis may be due to an occasional defect in DNA replication initiation on RNA primers. This defect is not absolute. Approximately 60 Okazaki fragments are made in the reaction with wt SSB during the 5-min reaction (~2500 nt Okazaki fragments synthesized at ~500 nt/s). Thus, repeated cycles of initiation, elongation and recycling to new primers occurs, even in the presence of the one-tailed SSB-LT-Drl. However, failure to reinitiate lagging strand synthesis likely leads to uncoupling of the reaction and possible replication fork collapse.

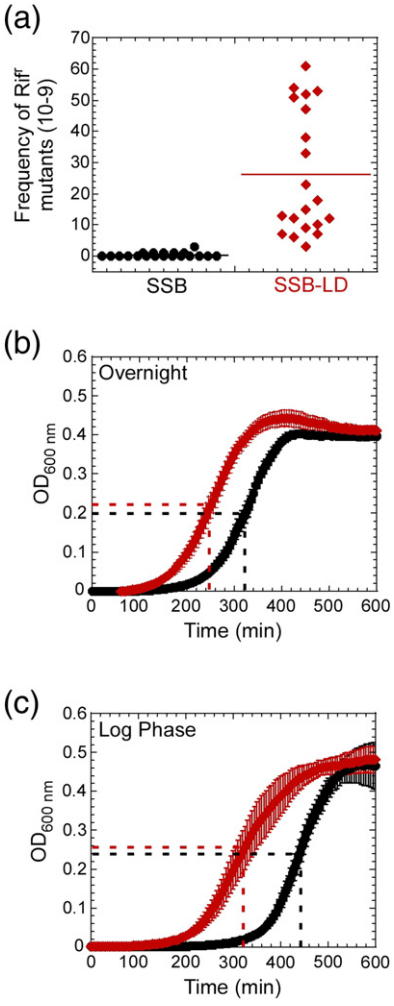

Fig. 7. Growth characteristics of *E. coli* cells carrying either four- or two-tailed SSB tetramers. (a) Rifampicin resistance assay showing the frequency of mutations in strains carrying the *wt SSB* or the *ssb-LD-Drl* genes. Growth analysis of *E. coli* cells with the *wt ssb* gene or *ssb-LD-Drl* gene shows faster recovery of the two-tailed SSB strain when the cultures are started from a overnight passage (b) or from a log phase starter culture (c).

Intuitively, the replication defects observed do not appear to be sufficiently severe to result in the dominant lethal phenotype observed for *ssb-LT-Drl*. Mechanisms exist in *E. coli* for reinitiation at collapsed initiation forks. The principal pathway proceeds through a PriA-dependent reaction. PriA recognizes collapsed forks and, through a reaction dependent on sequential interactions with PriB, DnaT and DnaC, leads to the reassembly of the DnaB helicase at forks and the ensuing re-entry of Pol III HE, re-establishing replication forks [73]. The PriA-dependent reaction is absolutely dependent upon SSB [64]. Thus, we sought to determine whether this replication restart reaction is impaired in the presence of SSB with less than the full complement of C-terminal tails.

We employed a FRET assay that monitors the separation of two strands by the DnaB helicase on artificial replication forks. Sterically blocking the 5′-end of the lagging strand template precludes helicase self-assembly by a threading reaction, making helicase PriA-, PriB-, DnaT-, DnaC- and SSB-dependent [64]. In the presence of SSB-LD-Drl, the reaction decreases to approximately 30%. However, in the presence of SSB-LT-Drl, the reaction is nearly completely inhibited.

An interaction between SSB and PriA is important for PriA function [22,31]. It is possible that multiple PriA monomers must interact with multiple C-terminal tails in a single SSB tetramer. The replication restart primosomal reaction involves sequential interactions of the PriA, PriB, DnaT and DnaC/DnaB proteins in a possible handoff reaction [74,75]. Thus, an SSB with multiple C-terminal tails could be required to bind to a partner downstream of PriA facilitating complex stability or requisite handoffs.

E. coli PriA mutants yield very small slow growing colonies and exhibit a low viability upon dilution and re-plating [73]. Viability could be due to a percentage of cells that do not experience replication fork collapse in sequential divisions. SSB-LT-Drl supports decreased levels of replication at reconstituted replication forks in reactions that likely lead to uncoupling and increased frequencies of replication fork collapse. That defect superimposed on the inability of cells to reinitiate by the PriA-dependent replication restart pathway provides a plausible explanation for the lethality observed with *ssb-LT-Drl*.

With respect to DNA repair, even though the levels of RecA protein are similar in cells expressing SSB-LD-Drl and wt SSB proteins upon exposure to DNA damage, the mutation frequency is 30-fold higher in cells expressing SSB-LD-Drl, the two-tailed

SSB variant. This may be due to an effect on SSB binding to the recombination mediator RecO. RecO, a part of the RecFOR mediator complex, binds directly to SSB and the RecFOR complex regulates the formation of the RecA nucleoprotein filament on ssDNA [76,77]. Apart from defective HR, the loss of interactions with other repair proteins such as RecQ, uracil DNA glycosylase and ExoI affect other pathways such as base excision repair and mismatch repair. Consequently, the lesions on the DNA are not repaired, leading to the higher frequency of mutagenesis. We propose that the inability of the SSB-LD-DrI tetramer at the replication fork to communicate the presence of the DNA lesion and deliver the DNA repair machinery might result in the absence of DNA repair. The results presented here highlight the significance of SSB and its SIP interacting C-terminal tails in mediating DNA replication and repair. It is interesting to note that *E. coli* cells carrying the *Dr*-SSB protein instead of the native wt *Ec*-SSB protein also show a higher frequency of spontaneous mutagenesis (Fig. S8). The *Dr*-SSB protein is not engineered and shows the same repair properties as the linked SSB-LD-DrI protein *in vivo*. This again suggests that the number of C-terminal tails on SSB influences coordination of DNA replication and repair in bacteria.

In bacterial cells, SSB functions at the interface of multiple biological processes including DNA replication, repair, recombination and replication restart. The number of C-terminal tails associated with each SSB tetramer appears to be a critical factor in regulating how these processes function and are coupled.

Materials and methods

Cloning of linked SSBs

The *wt ssb* gene was cloned into a pET-21a protein expression vector (EMD, Germany) with NdeI and BamHI restriction sites flanking its coding region. The detailed methodology to generate the linked SSBs is described in the supplemental information section.

Protein purification

The wt SSB, ssb-S1 and deletion constructs were purified as previously described for wt SSB [78,79], and all the buffers included a 1× final concentration of the protease inhibitor cocktail (Sigma, Missouri). The linked SSBs were purified using a slightly modified procedure as described in the supplemental materials. DNA replication proteins, β_2 [80], $DnaB_6$ [81] and DnaG [82] were purified as previously described. DNA polymerase III* (Pol $III_3\tau_2\gamma\delta\delta'\chi\psi$) was purified as previously described [83] from overexpressing cells that contained a plasmid bearing an artificial operon containing all of the Pol III* subunit genes. Primosomal proteins PriA, $PriB_2$, $DnaT_3$ and DnaC were obtained using a published strategy [81] with modifications (Yuan and McHenry, unpublished results).

DNA

The oligodeoxynucleotides, $(dT)_{35}$ and $(dT)_{70}$, were synthesized and purified as previously described [16]. Poly(dT) was purchased from Midland Certified Reagent Company (Midland, TX) and dialyzed extensively against buffer using dialysis membrane with a 3500-Da molecular mass cutoff (Spectrum Inc., Houston, TX). All ssDNA concentrations were determined spectrophotometrically using the extinction coefficient $\varepsilon_{260} = 8.1 \times 10^3\ M^{-1}$ (nt) cm^{-1} for oligo(dT) and poly(dT) [84]. Mini-circle DNA templates were 409-nt duplex circles with a 396-nt single-stranded tail that served as the initial lagging strand template [85]. The leading and lagging strands had a 50:1 asymmetric G:C distribution, allowing quantification of leading and lagging strand synthesis by [^{32}P]dCTP and dGTP incorporation, respectively. DNA was prepared as previously described [85] with modifications (Yuan and McHenry, unpublished results).

Analytical sedimentation

Sedimentation velocity and equilibrium experiments were performed using an Optima XL-A analytical ultracentrifuge equipped with an An50Ti rotor (Beckman Coulter, Fullerton, CA) at 25 °C. For sedimentation velocity experiments in Fig. 1c, we measured the sedimentation properties of 1 μM SSB (four OB-folds) in 30 mM Tris–Cl, pH 8.0, 10% glycerol, 0.2 M NaCl and 1 mM EDTA. We loaded 380 μl of the sample and 392 μl of the buffer into their appropriate sectors of an Epon charcoal-filled two-sector centerpiece and centrifuged them at 42,000 rpm (25 °C) while the absorbance was monitored at 280 nm. The continuous sedimentation coefficient $c(s)$ was calculated using the program SEDFIT [86,87]. For sedimentation equilibrium experiments (Fig. 1d and e), 120 μl of protein solution was loaded into each of the three channels of an Epon charcoal-filled six-channel centerpiece with 130 μl of buffer in each reference channels. Protein concentration was monitored by absorbance at 280 nm (SSB-LD-DrI) and 230 nm (SSB-LT-DrI) at three different protein concentrations ([SSB-LD-DrI] = 3.6 μM, 2.3 μM and 1 μM; [SSB-LT-DrI] = 2.2 μM, 1.2 μM and 0.6 μM). Data were collected with a spacing of 0.001 cm with an average of 10 scans per step at four rotor speeds: 9500, 11,500, 14,000 and 17,000 rpm. At each speed, sedimentation equilibrium was determined when successive scans measured over a 2-h time window were superimposable. Data sets were edited and extracted using SEDFIT [86,87] followed by analysis by nonlinear least squares using the program SEDPHAT [88]. Apparent molecular weights were obtained by fitting the data to Eq. (1):

$$A_T = \sum_{i=1}^{n} \exp\left(\ln A_{0,i} + \sigma_i\left(r^2 - r_{ref}^2\right)/2\right) + b \qquad (1)$$

where A_T is the total absorbance at radial position r, $A_{0,i}$ is the absorbance of component i at the reference radial position (r_{ref}), b is the baseline offset, $\sigma_i = [M_i(1-\bar{\vartheta}_u\rho)\omega^2]/RT$ and M_i

and $\upsilon\bar{\vartheta}_i$ are the molecular mass and partial specific volume of component *i*, respectively (calculated using SEDENTREP [89]). For *Pf*-SSB, the $\upsilon\bar{\vartheta}_i$ value (0.7191 ml/g at 25 °C) was calculated based on its amino acid composition (residues 77–284). The solution density ρ for buffer $H^{0.1M}$ was 1.0026 (calculated using SEDENTREP). ω is the angular velocity, *R* is the ideal gas constant and *T* is the absolute temperature. A global nonlinear least squares fit to Eq. (1) of the nine absorbance files was used to calculate the molecular weight.

Fluorescence titrations

Equilibrium binding of SSB to oligodeoxynucleotides poly(dT) and $(dT)_L$ was performed by monitoring the quenching of intrinsic SSB tryptophan fluorescence upon addition of DNA (PTI-QM-2000 spectrofluorometer; PTI Inc., Lawrenceville, NJ) [λ_{ex} = 296 nm (2-nm bandpass) and λ_{em} = 345 nm (2- to 5-nm bandpass)] with corrections applied as previously described [16]. Experiments were carried out at 25 °C in Buffer T: 10 mM Tris–Cl, pH 8.1, 0.1 mM EDTA and [NaCl] varied as noted in the text.

Wrapping experiment

Wrapping of ssDNA around the SSB tetramer was measured on a deoxyoligonucleotide 65 nt in length with a Cy5.5 fluorophore at the 5′-end and a Cy3 fluorophore at the 3′-end. We incubated 50 nM DNA with increasing [SSB], and the enhancement of Cy5.5 fluorescence was monitored at 700 nm by exciting the Cy3 probe at 515 nm. These experiments were performed at 25 °C.

In vivo bumping experiments

Bumping experiments were performed as described previously [90]. *RPD317* is a strain where the chromosomal *ssb* gene has been deleted, but the strains survive using a copy of the *ssb* gene on a helper plasmid with a *Tet*^{r} cassette. We transformed these cells with our test SSB containing plasmid carrying the *Amp*^{r} cassette. We selected transformants that grew on the LB agar plates with ampicillin (Amp, 100 μg/ml) and kanamycin (Kan, 50 μg/ml) and passaged them six times in 5-ml LB media containing Amp + Kan. For each passage, the cells were grown overnight for 16 h at 37 °C with shaking at 250 rpm. After the final passage, the cells were diluted 1:1000 and plated onto LB agar containing Kan + Amp or Kan + Tet (34 g/ml tetracycline). Strains that can complement loss of *SSB-WT* grew only on the plates with Amp + Kan whereas those that did not complement grew on plates with either Kan + Amp or Kan + Tet because they could not bump the functional version of the wt *SSB* protein. For all the experiments, a plasmid containing wt *ssb* was used as a control to monitor the efficiency of bumping. All the bumping results were repeated at least twice and identical results were obtained.

In vitro single-stranded replication assay

We incubated 0.8 μM SSB_4 with 2.3 nM M13Gori ssDNA annealed with a 30-nt primer, 15 nM β_2 and 2 nM Pol III* in the presence of 0.1 mM ATP, 18 μM [^{3}H]dTTP (100 cpm/pmol total nucleotide), 48 μM dATP, 48 μM dGTP and 48 μM dCTP at 30 °C for the indicated time periods. The ssDNA replication buffer contains 10 mM magnesium acetate, 200 mM NaCl, 50 mM Hepes (pH 7.5), 100 mM potassium glutamate, 20% glycerol, 200 μg/ml bovine serum albumin, 0.02% Nonidet P-40 and 10 mM dithiothreitol. Reactions were quenched, and products were quantified by scintillation counting as previously described [28].

In vitro rolling circle replication assays

We incubated 20 nM mini-circle DNA template, the designated level of SSB_4, 100 nM β_2, 12 nM $DnaB_6$, 100 nM DnaG, 2.5 nM Pol III*, 160 nM PriA, 50 nM $PriB_2$, 333 nM $DnaT_3$ and 108 nM DnaC with 5 μM ATPγS, 200 μM CTP, 200 μM UTP and 200 μM GTP for 5 min at 30 °C. The reaction buffer was the same as in the single-stranded replication assay except that 50 or 25 mM NaCl (contributed by 0.8 μM or 0.4 μM SSB_4, respectively) was used instead of 200 mM. We added 1 mM ATP and 100 μM dNTPs to start the reaction. After 3 min, [α-^{32}P] dCTP or dGTP was added to allow quantification of leading and lagging strand synthesis, respectively. The reaction was quenched with an equal volume of stop mix [40 mM Tris–HCl (pH 8.0), 0.2% SDS, 100 mM EDTA and 50 μg/ml proteinase K] after 5 min. DNA product was quantified as in the single-stranded replication assays [28]. For the analysis of the size of lagging strand products, samples were mixed with 30 mM NaOH, 2 mM EDTA, 2% glycerol and 0.02% bromophenol blue and were fractionated on 0.6% alkaline agarose gels for approximately 18 h at 24 V in a running buffer of 30 mM NaOH and 2 mM EDTA. Gels were fixed in 8% (w/v) trichloroacetic acid, dried onto DEAE paper, imaged on storage phosphor screens and scanned with a PhosphorImager. The lengths of Okazaki fragment (*L*) were determined by a method that removed the bias of more radioactivity being incorporated into longer products using $L = \sum(L_i \times n_i)/\sum n_i$, where n_i is the relative molar amount of the Okazaki fragments with a certain length L_i. $n_i = \text{density}_i/L_i$, where density_i is the pixel density at L_i in a lane determined using ImageQuant. Thus, $L = \sum\text{density}_i/\sum(\text{density}_i/\text{length}_i)$.

FRET replication restart assay

This assay was conducted as previously described [64]. We combined 20 nM substrate constructed from FT_{90}, QT_{90} and P_{10g} with 100 nM trap oligo (45-mer complimentary to duplex region of FT_{90}), 200 nM streptavidin and protein components in a buffer containing 50 mM Hepes (pH 7.5), 10 mM magnesium acetate, 10 mM dithiothreitol, 20% (v/v) glycerol, 0.02% (v/v) Nonidet P-40 detergent, 200 μg/ml bovine serum albumin, 100 mM potassium glutamate and 10 mM ATP in a round-bottomed black 96-well plate in a final volume of 50 μl. Samples were incubated at 30 °C for 15 min. Fluorescence emission was detected at 535 nm using an Envision plate reader with an excitation of 485 nm. Using concentrations of un-annealed fluorescent leading strand template that are in the linear range of the assay, we converted fluorescent units to molarity using a standard curve.

DNA damage experiments

Effect of HU and HN2

A 5-ml culture of *RDP317* cells with either *wt ssb* or *ssb-LD-Drl* under control of the native *ssb* promoter was grown to an OD_{600} of 0.2 in the presence of 50 μg/ml kanamycin and 100 μg/ml ampicillin. HU was added to the cultures (final concentration, 100 mM) and grown for an additional 5 h at 37 °C. The cells were harvested and washed five times with 5 ml of ice-cold phosphate-buffered saline (PBS). After the final wash, the cells were resuspended in 10 ml of 1× PBS, and five serial dilutions were generated. We plated 4 μl from each dilution in the series onto LB and grown overnight at 37 °C. To quantitate the effect of nitrogen mustard (HN2), we grew cells carrying either the wt *ssb* or the *ssb–LD-Drl* genes as for the HU experiment and we added 2 mM HN2 (final concentration) to the cells when the OD_{600} reached 0.5. The cells were grown for another hour at 37 °C, and 1 ml of this culture was directly diluted into 10 ml of M9 media. Serial dilutions were generated and immediately plated onto LB agar media containing 100 μg/ml of ampicillin and 50 μg/ml of kanamycin.

UV sensitivity

RDP317 cells with either *wt ssb* or *ssb-LD-Drl* under control of the native SSB promoter were grown overnight, and 5-fold serial dilutions of these cells were made and 4 μl of the dilutions was spotted on a LB plate carrying 50 μg/ml kanamycin. The plates were dried for 30 min at 37 °C and exposed to UV.

RecA Western blot

RDP317 cells with either *wt ssb* or *ssb-LD-Drl* under control of the native SSB promoter were grown to an OD_{600} of 0.5 in the presence of both 100 μg/ml ampicillin and 50 μg/ml kanamycin. Nalidixic acid was added to the cultures (final concentration was 100 μg/ml) followed by growth at 37 °C. We removed 1 ml of the sample at the appropriate time intervals (30, 60, 90 and 120 min) and spun it down using a table top centrifuge, and the cells were washed three times with 1.5 ml of ice-cold PBS. We resolved 50 μg of the total cell lysate collected at each time point on a 10% SDS-PAGE gel followed by Western blotting. We used a 1:15,000 ration of the anti-RecA antibody (MD-03-3; MBL Corp., Massachusetts, USA) and detected the levels of RecA using chemiluminescence.

Rifampicin resistance

To measure the rate of spontaneous mutagenesis of the RDP317 cells carrying either the *wt ssb* or the *ssb-LD-Drl* genes, we grew overnight cultures of these cells in the presence of 100 μg/ml ampicillin and 50 μg/ml kanamycin. The cultures were then plated onto LB agar media, 20 colonies were picked for each strain and 5-ml cultures for each colony were grown overnight at 37 °C. The cultures were then plated onto LB agar media containing 10 μg/ml rifampicin (Sigma). The plates were incubated overnight at 37 °C, and the numbers of colonies were counted. The experiment was repeated three times, and the mutagenesis of 20 individual colonies was screened during each trial.

Growth curves

To measure the growth kinetics of RDP317 cells carrying either the *wt ssb* or *ssb*-LD-Drl genes, we selected 8 colonies from each plate and either grew an overnight culture or to an OD_{600} of 0.6. We diluted 1 μl from each of these starting conditions to 1 ml of fresh LB with 100 μg/ml ampicillin and 50 μg/ml of kanamycin. We added 200 μl of this diluted culture into a 96-well Greiner cell culture plate (USA Scientific, Cat No. 655180), and the cells were grown in a Tecan infinite M200 pro plate reader (Tecan Systems, California, USA) with constant shaking at 250 rpm. The OD_{600} was measured every 10 min and plotted *versus* time to generate the growth curves.

Acknowledgements

We thank Thang Ho for assistance with DNA synthesis, Dr. Peter Burgers for extensive technical advice and invaluable suggestions and Dr. Ron Porter for the RDP317 strain. We also thank Drs. Vasanth Muralitharan and Sofia Origanti for assistance with the Western blotting, Dr. Michael Caparon for use of the Tecan plate reader and Dr. Vince Waldman for comments on the manuscript. This work was supported by grants from the National Institutes of Health GM30498 to T.M.L. and National Science Foundation to C.S.M.

Appendix A. Supplementary data

Supplementary data to this article can be found online at http://dx.doi.org/10.1016/j.jmb.2013.08.021

Received 13 June 2013;
Received in revised form 1 August 2013;
Accepted 16 August 2013
Available online 7 September 2013

Keywords:
single stranded DNA binding protein;
SSB;
DNA replication;
DNA repair;
DNA binding

3 Present Address: E. Antony, Department of Chemistry and Biochemistry, Utah State University, 0300 Old Main Hill, Logan, UT 84322, USA.

Abbreviations used:
SSB, single-stranded DNA binding protein; EDTA, ethylenediaminetetraacetic acid; PBS, phosphate-buffered saline; FRET, fluorescence resonance energy transfer; ssDNA, single-stranded DNA; SIP, SSB interacting protein; wt, wild type.

References

[1] Chase JW, Williams KR. Single-stranded DNA binding proteins required for DNA replication. Annu Rev Biochem 1986;55:103–36.

[2] Meyer RR, Laine PS. The single-stranded DNA-binding protein of *Escherichia coli*. Microbiol Rev 1990;54:342–80.

[3] Lohman TM, Ferrari ME. *Escherichia coli* single-stranded DNA-binding protein: multiple DNA-binding modes and cooperativities. Annu Rev Biochem 1994;63:527–70.

[4] Williams KR, Spicer EK, LoPresti MB, Guggenheimer RA, Chase JW. Limited proteolysis studies on the *Escherichia coli* single-stranded DNA binding protein. Evidence for a functionally homologous domain in both the *Escherichia coli* and T4 DNA binding proteins. J Biol Chem 1983;258:3346–55.

[5] Raghunathan S, Kozlov AG, Lohman TM, Waksman G. Structure of the DNA binding domain of *E. coli* SSB bound to ssDNA. Nat Struct Biol 2000;7:648–52.

[6] Raghunathan S, Ricard CS, Lohman TM, Waksman G. Crystal structure of the homo-tetrameric DNA binding domain of *Escherichia coli* single-stranded DNA-binding protein determined by multiwavelength X-ray diffraction on the selenomethionyl protein at 2.9-Å resolution. Proc Natl Acad Sci USA 1997;94:6652–7.

[7] Shereda RD, Kozlov AG, Lohman TM, Cox MM, Keck JL. SSB as an organizer/mobilizer of genome maintenance complexes. Crit Rev Biochem Mol Biol 2008;43:289–318.

[8] Bujalowski W, Lohman TM. *Escherichia coli* single-strand binding protein forms multiple, distinct complexes with single-stranded DNA. Biochemistry 1986;25:7799–802.

[9] Chrysogelos S, Griffith J. *Escherichia coli* single-strand binding protein organizes single-stranded DNA in nucleosome-like units. Proc Natl Acad Sci USA 1982;79:5803–7.

[10] Lohman TM, Overman LB. Two binding modes in *Escherichia coli* single strand binding protein-single stranded DNA complexes. Modulation by NaCl concentration. J Biol Chem 1985;260:3594–603.

[11] Griffith JD, Harris LD, Register J. Visualization of SSB-ssDNA complexes active in the assembly of stable RecA-DNA filaments. Cold Spring Harbor Symp Quant Biol 1984;49:553–9.

[12] Lohman TM, Bujalowski W, Overman LB, Wei TF. Interactions of the *E. coli* single strand binding (SSB) protein with ss nucleic acids. Binding mode transitions and equilibrium binding studies. Biochem Pharmacol 1988;37:1781–2.

[13] Lohman TM, Overman LB, Datta S. Salt-dependent changes in the DNA binding co-operativity of *Escherichia coli* single strand binding protein. J Mol Biol 1986;187:603–15.

[14] Zhou R, Kozlov AG, Roy R, Zhang J, Korolev S, Lohman TM, et al. SSB functions as a sliding platform that migrates on DNA via reptation. Cell 2011;146:222–32.

[15] Roy R, Kozlov AG, Lohman TM, Ha T. SSB protein diffusion on single-stranded DNA stimulates RecA filament formation. Nature 2009;461:1092–7.

[16] Ferrari ME, Bujalowski W, Lohman TM. Co-operative binding of *Escherichia coli* SSB tetramers to single-stranded DNA in the (SSB)35 binding mode. J Mol Biol 1994;236:106–23.

[17] Kozlov AG, Lohman TM. Kinetic mechanism of direct transfer of *Escherichia coli* SSB tetramers between single-stranded DNA molecules. Biochemistry 2002;41:11611–27.

[18] Bujalowski W, Overman LB, Lohman TM. Binding mode transitions of *Escherichia coli* single strand binding protein-single-stranded DNA complexes. Cation, anion, pH, and binding density effects. J Biol Chem 1988;263:4629–40.

[19] Lohman TM, Bujalowski W, Overman LB. *E. coli* single strand binding protein: a new look at helix-destabilizing proteins. Trends Biochem Sci 1988;13:250–5.

[20] McHenry CS. DNA replicases from a bacterial perspective. Annu Rev Biochem 2011;80:403–36.

[21] Naue N, Curth U. Investigation of protein–protein interactions of single-stranded DNA-binding proteins by analytical ultracentrifugation. Methods Mol Biol 2012;922:133–49.

[22] Kozlov AG, Jezewska MJ, Bujalowski W, Lohman TM. Binding specificity of *Escherichia coli* single-stranded DNA binding protein for the chi subunit of DNA pol III holoenzyme and PriA helicase. Biochemistry 2010;49:3555–66.

[23] Glover BP, McHenry CS. The chi psi subunits of DNA polymerase III holoenzyme bind to single-stranded DNA-binding protein (SSB) and facilitate replication of an SSB-coated template. J Biol Chem 1998;273:23476–84.

[24] Kelman Z, Yuzhakov A, Andjelkovic J, O'Donnell M. Devoted to the lagging strand-the subunit of DNA polymerase III holoenzyme contacts SSB to promote processive elongation and sliding clamp assembly. EMBO J 1998;17:2436–49.

[25] Downey CD, McHenry CS. Chaperoning of a replicative polymerase onto a newly assembled DNA-bound sliding clamp by the clamp loader. Mol Cell 2010;37:481–91.

[26] Marceau AH, Bahng S, Massoni SC, George NP, Sandler SJ, Marians KJ, et al. Structure of the SSB-DNA polymerase III interface and its role in DNA replication. EMBO J 2011;30:4236–47.

[27] Quinones A, Neumann S. The ssb-113 allele suppresses the dnaQ49 mutator and alters DNA supercoiling in *Escherichia coli*. Mol Microbiol 1997;25:237–46.

[28] Yuan Q, McHenry CS. Strand displacement by DNA polymerase III occurs through a tau-psi-chi link to single-stranded DNA-binding protein coating the lagging strand template. J Biol Chem 2009;284:31672–9.

[29] Yuzhakov A, Kelman Z, O'Donnell M. Trading places on DNA—a three-point switch underlies primer handoff from primase to the replicative DNA polymerase. Cell 1999;96:153–63.

[30] Naue N, Beerbaum M, Bogutzki A, Schmieder P, Curth U. The helicase-binding domain of *Escherichia coli* DnaG primase interacts with the highly conserved C-terminal region of single-stranded DNA-binding protein. Nucleic Acids Res 2013;41:4507–17.

[31] Cadman CJ, McGlynn P. PriA helicase and SSB interact physically and functionally. Nucleic Acids Res 2004;32:6378–87.

[32] Cadman CJ, Lopper M, Moon PB, Keck JL, McGlynn P. PriB stimulates PriA helicase via an interaction with single-stranded DNA. J Biol Chem 2005;280:39693–700.

[33] Lecointe F, Serena C, Velten M, Costes A, McGovern S, Meile JC, et al. Anticipating chromosomal replication fork arrest: SSB targets repair DNA helicases to active forks. EMBO J 2007;26:4239–51.

[34] Shereda RD, Bernstein DA, Keck JL. A central role for SSB in *Escherichia coli* RecQ DNA helicase function. J Biol Chem 2007;282:19247–58.
[35] Han ES, Cooper DL, Persky NS, Sutera VA, Whitaker RD, Montello ML, et al. RecJ exonuclease: substrates, products and interaction with SSB. Nucleic Acids Res 2006;34:1084–91.
[36] Lu D, Myers AR, George NP, Keck JL. Mechanism of exonuclease I stimulation by the single-stranded DNA-binding protein. Nucleic Acids Res 2011;39:6536–45.
[37] Umezu K, Kolodner RD. Protein interactions in genetic recombination in *Escherichia coli*. Interactions involving RecO and RecR overcome the inhibition of RecA by single-stranded DNA-binding protein. J Biol Chem 1994;269:30005–13.
[38] Furukohri A, Nishikawa Y, Akiyama MT, Maki H. Interaction between *Escherichia coli* DNA polymerase IV and single-stranded DNA-binding protein is required for DNA synthesis on SSB-coated DNA. Nucleic Acids Res 2012;40:6039–48.
[39] Kowalczykowski SC, Dixon DA, Eggleston AK, Lauder SD, Rehrauer WM. Biochemistry of homologous recombination in *Escherichia coli*. Microbiol Rev 1994;58:401–65.
[40] Shereda RD, Reiter NJ, Butcher SE, Keck JL. Identification of the SSB binding site on *E. coli* RecQ reveals a conserved surface for binding SSB's C terminus. J Mol Biol 2009;386:612–25.
[41] Handa P, Acharya N, Varshney U. Chimeras between single-stranded DNA-binding proteins from *Escherichia coli* and *Mycobacterium tuberculosis* reveal that their C-terminal domains interact with uracil DNA glycosylases. J Biol Chem 2001;276:16992–7.
[42] Molineux IJ, Gefter ML. Properties of the *Escherichia coli* in DNA binding (unwinding) protein: interaction with DNA polymerase and DNA. Proc Natl Acad Sci USA 1974;71:3858–62.
[43] Arad G, Hendel A, Urbanke C, Curth U, Livneh Z. Single-stranded DNA-binding protein recruits DNA polymerase V to primer termini on RecA-coated DNA. J Biol Chem 2008;283:8274–82.
[44] Bernstein DA, Eggington JM, Killoran MP, Misic AM, Cox MM, Keck JL. Crystal structure of the *Deinococcus radiodurans* single-stranded DNA-binding protein suggests a mechanism for coping with DNA damage. Proc Natl Acad Sci USA 2004;101:8575–80.
[45] Fedorov R, Witte G, Urbanke C, Manstein DJ, Curth U. 3D structure of *Thermus aquaticus* single-stranded DNA-binding protein gives insight into the functioning of SSB proteins. Nucleic Acids Res 2006;34:6708–17.
[46] Kozlov AG, Eggington JM, Cox MM, Lohman TM. Binding of the dimeric *Deinococcus radiodurans* single-stranded DNA binding protein to single-stranded DNA. Biochemistry 2010;49:8266–75.
[47] Witte G, Urbanke C, Curth U. Single-stranded DNA-binding protein of *Deinococcus radiodurans*: a biophysical characterization. Nucleic Acids Res 2005;33:1662–70.
[48] George NP, Ngo KV, Chitteni-Pattu S, Norais CA, Battista JR, Cox MM, et al. Structure and cellular dynamics of *Deinococcus radiodurans* single-stranded DNA (ssDNA)-binding protein (SSB)-DNA complexes. J Biol Chem 2012;287:22123–32.
[49] Roy R, Kozlov AG, Lohman TM, Ha T. Dynamic structural rearrangements between DNA binding modes of *E. coli* SSB protein. J Mol Biol 2007;369:1244–57.
[50] Bujalowski W, Lohman TM. Negative co-operativity in *Escherichia coli* single strand binding protein-oligonucleotide interactions. II. Salt, temperature and oligonucleotide length effects. J Mol Biol 1989;207:269–88.
[51] Kozlov AG, Lohman TM. Stopped-flow studies of the kinetics of single-stranded DNA binding and wrapping around the *Escherichia coli* SSB tetramer. Biochemistry 2002;41:6032–44.
[52] Bujalowski W, Lohman TM. Negative co-operativity in *Escherichia coli* single strand binding protein-oligonucleotide interactions. I. Evidence and a quantitative model. J Mol Biol 1989;207:249–68.
[53] Lohman TM, Bujalowski W. Negative cooperativity within individual tetramers of *Escherichia coli* single strand binding protein is responsible for the transition between the (SSB)35 and (SSB)56 DNA binding modes. Biochemistry 1988;27:2260–5.
[54] Porter RD, Black S. The single-stranded-DNA-binding protein encoded by the *Escherichia coli* F factor can complement a deletion of the chromosomal ssb gene. J Bacteriol 1991;173:2720–3.
[55] Wadood A, Dohmoto M, Sugiura S, Yamaguchi K. Characterization of copy number mutants of plasmid pSC101. J Gen Appl Microbiol 1997;43:309–16.
[56] Yamaguchi K. Replication of plasmid DNA. Radioisotopes 1984;33:307–14.
[57] Curth U, Genschel J, Urbanke C, Greipel J. *In vitro* and *in vivo* function of the C-terminus of *Escherichia coli* single-stranded DNA binding protein. Nucleic Acids Res 1996;24:2706–11.
[58] Dallmann HG, Kim S, Pritchard AE, Marians KJ, McHenry CS. Characterization of the unique C terminus of the *Escherichia coli* tau DnaX protein. Monomeric C-tau binds alpha AND DnaB and can partially replace tau in reconstituted replication forks. J Biol Chem 2000;275:15512–9.
[59] Gao D, McHenry CS. tau binds and organizes *Escherichia coli* replication proteins through distinct domains. Domain IV, located within the unique C terminus of tau, binds the replication fork, helicase, DnaB. J Biol Chem 2001;276:4441–6.
[60] Kim S, Dallmann HG, McHenry CS, Marians KJ. Coupling of a replicative polymerase and helicase: a tau-DnaB interaction mediates rapid replication fork movement. Cell 1996;84:643–50.
[61] Tougu K, Marians KJ. The interaction between helicase and primase sets the replication fork clock. J Biol Chem 1996;271:21398–405.
[62] Tougu K, Marians KJ. The extreme C terminus of primase is required for interaction with DnaB at the replication fork. J Biol Chem 1996;271:21391–7.
[63] Zechner EL, Wu CA, Marians KJ. Coordinated leading- and lagging-strand synthesis at the *Escherichia coli* DNA replication fork. III. A polymerase-primase interaction governs primer size. J Biol Chem 1992;267:4054–63.
[64] Manhart CM, McHenry CS. The PriA replication restart protein blocks replicase access prior to helicase assembly and directs template specificity through its ATPase activity. J Biol Chem 2013;288:3989–99.
[65] Costes A, Lecointe F, McGovern S, Quevillon-Cheruel S, Polard P. The C-terminal domain of the bacterial SSB protein acts as a DNA maintenance hub at active chromosome replication forks. PLoS Genet 2010;6:e1001238.
[66] Rosenkranz HS, Garro AJ, Levy JA, Carr HS. Studies with hydroxyurea. I. The reversible inhibition of bacterial DNA synthesis and the effect of hydroxyurea on the bactericidal action of streptomycin. Biochim Biophys Acta 1966;114:501–15.
[67] Rosenkranz HS, Levy JA. Hydroxyurea: a specific inhibitor of deoxyribonucleic acid synthesis. Biochim Biophys Acta 1965;95:181–3.

[68] Biesele JJ, Philips FS, Thiersch JB, Burchenal JH, Buckley SM, Stock CC, et al. Chromosome alteration and tumour inhibition by nitrogen mustards; the hypothesis of cross-linking alkylation. Nature 1950;166:1112–4.
[69] Bonura T, Smith KC. Enzymatic production of deoxyribonucleic acid double-strand breaks after ultraviolet irradiation of *Escherichia coli* K-12. J Bacteriol 1975;121:511–7.
[70] Ezekiel DH, Hutchins JE. Mutations affecting RNA polymerase associated with rifampicin resistance in *Escherichia coli*. Nature 1968;220:276–7.
[71] Rosenberg SM. Evolving responsively: adaptive mutation. Nat Rev Genet 2001;2:504–15.
[72] Zechner EL, Wu CA, Marians KJ. Coordinated leading- and lagging-strand synthesis at the *Escherichia coli* DNA replication fork. II. Frequency of primer synthesis and efficiency of primer utilization control Okazaki fragment size. J Biol Chem 1992;267:4045–53.
[73] Marians KJ. PriA-directed replication fork restart in *Escherichia coli*. Trends Biochem Sci 2000;25:185–9.
[74] Liu J, Nurse P, Marians KJ. The ordered assembly of the phiX174-type primosome. III. PriB facilitates complex formation between PriA and DnaT. J Biol Chem 1996;271:15656–61.
[75] Lopper M, Boonsombat R, Sandler SJ, Keck JL. A hand-off mechanism for primosome assembly in replication restart. Mol Cell 2007;26:781–93.
[76] Morimatsu K, Wu Y, Kowalczykowski SC. RecFOR proteins target RecA protein to a DNA gap with either DNA or RNA at the 5′ terminus: implication for repair of stalled replication forks. J Biol Chem 2012;287:35621–30.
[77] Sakai A, Cox MM. RecFOR and RecOR as distinct RecA loading pathways. J Biol Chem 2009;284:3264–72.
[78] Bujalowski W, Lohman TM. Monomers of the *Escherichia coli* SSB-1 mutant protein bind single-stranded DNA. J Mol Biol 1991;217:63–74.
[79] Lohman TM. Kinetics of protein-nucleic acid interactions: use of salt effects to probe mechanisms of interaction. CRC Crit Rev Biochem 1986;19:191–245.
[80] Johanson KO, Haynes TE, McHenry CS. Chemical characterization and purification of the beta subunit of the DNA polymerase III holoenzyme from an overproducing strain. J Biol Chem 1986;261:11460–5.
[81] Marians KJ. Phi X174-type primosomal proteins: purification and assay. Methods Enzymol 1995;262:507–21.
[82] Griep MA, McHenry CS. Glutamate overcomes the salt inhibition of DNA polymerase III holoenzyme. J Biol Chem 1989;264:11294–301.
[83] Fay PJ, Johanson KO, McHenry CS, Bambara RA. Size classes of products synthesized processively by two subassemblies of *Escherichia coli* DNA polymerase III holoenzyme. J Biol Chem 1982;257:5692–9.
[84] Kowalczykowski SC, Lonberg N, Newport JW, von Hippel PH. Interactions of bacteriophage T4-coded gene 32 protein with nucleic acids. I. Characterization of the binding interactions. J Mol Biol 1981;145:75–104.
[85] Sanders GM, Dallmann HG, McHenry CS. Reconstitution of the B. subtilis replisome with 13 proteins including two distinct replicases. Mol Cell 2010;37:273–81.
[86] Schuck P. Sedimentation analysis of noninteracting and self-associating solutes using numerical solutions to the Lamm equation. Biophys J 1998;75:1503–12.
[87] Dam J, Schuck P. Calculating sedimentation coefficient distributions by direct modeling of sedimentation velocity concentration profiles. Methods Enzymol 2004;384:185–212.
[88] Vistica J, Dam J, Balbo A, Yikilmaz E, Mariuzza RA, Rouault TA, et al. Sedimentation equilibrium analysis of protein interactions with global implicit mass conservation constraints and systematic noise decomposition. Anal Biochem 2004;326:234–56.
[89] Laue TM, Shah BD, RIdgeway TM, Pelletier SL. Computer-aided interpretation of analytical sedimentation data for proteins. Cambridge, UK: Royal Society of Cambridge; 1992 [1].
[90] Porter RD, Black S, Pannuri S, Carlson A. Use of the *Escherichia coli* SSB gene to prevent bioreactor takeover by plasmidless cells. Biotechnology 1990;8:47–51.